Atmospheric Research 149 (2014) 77–87

Contents lists available at ScienceDirect

Atmospheric Research

journal homepage: www.elsevier.com/locate/atmos

Supercooled liquid water content profiling case studies with a new vibrating wire sonde compared to a ground-based microwave radiometer

David Serke [a,*], Emrys Hall [b,c], John Bognar [d], Allen Jordan [b,c], Spencer Abdo [d], Kirstin Baker [d], Tom Seitel [d], Marta Nelson [e], Randolph Ware [c,e,f], Frank McDonough [a], Marcia Politovich [a]

[a] National Center for Atmospheric Research, Research Applications Laboratory, Boulder, CO 80301, USA
[b] NOAA ESRL Global Monitoring Division, Boulder, CO 80305, USA
[c] Cooperative Institute for Research in Environmental Sciences, University of Colorado, Boulder, CO 80309, USA
[d] Anasphere Inc., Bozeman, MT 59718, USA
[e] Radiometrics Corporation, Boulder, CO 80301, USA
[f] National Center for Atmospheric Research, Earth Observation Laboratory, Boulder, CO 80301, USA

ARTICLE INFO

Article history:
Received 11 March 2014
Received in revised form 29 May 2014
Accepted 30 May 2014
Available online 6 June 2014

Keywords:
In-flight icing
Supercooled liquid water
Aviation hazard
Radiosonde profile
Microwave radiometer

ABSTRACT

An improved version of the vibrating wire sensor, used to measure supercooled cloud liquid water content, was developed by Anasphere Inc. and tested during early 2012. The sensor works on the principle that supercooled liquid will freeze to the vibrating wire and reduce the frequency at a known rate proportional to the liquid water content as the sensor rises through the cloud attached to a weather balloon and radiosonde. The disposable Anasphere sensor interfaces with an InterMet Systems iMet radiosonde. This updated sensor reduces the weight of the instrument while updating the technology when compared to the preceding balloon-borne sensor that was developed in the 1980's by Hill and Woffinden.

Balloon-borne test flights were performed from Boulder, Colorado during February and March of 2012. These flights provided comparisons to integrated liquid water and profiles of liquid water content derived from a collocated multichannel microwave radiometer, built and operated by Radiometrics Corporation. Inter-comparison data such as these are invaluable for calibration, verification and validation of remote-sensing instruments. The data gathered from this sensor are potentially important to detection of icing hazards to aircraft, validation of microphysical output from numerical models, and calibrating remote sensors measuring supercooled liquid water.

1. Introduction

Liquid water existing within subfreezing temperature profiles is said to be 'supercooled liquid water' (SLW). When an aircraft encounters SLW, the SLW freezes quickly onto the leading edges, which acts to increase drag and reduce lift. SLW drops above 50 μm in diameter, termed 'supercooled large drops', can be even more dangerous to flight as they tend to splash and roll back beyond the aircraft's leading edges where icing defenses such as heaters or boots are located. For these

* Corresponding author. Tel.: +1 303 618 9770.
E-mail addresses: serke@ucar.edu (D. Serke), emrys.hall@noaa.gov (E. Hall), jbognar@anasphere.com (J. Bognar), allen.jordan@noaa.gov (A. Jordan), sabdo@anasphere.com (S. Abdo), kbaker@anasphere.com (K. Baker), tseitel@anasphere.com (T. Seitel), marta.nelson@radiometrics.com (M. Nelson), randolph.ware@gmail.com (R. Ware), frankmcdonough.wx@gmail.com (F. McDonough), marcia@ucar.edu (M. Politovich).

http://dx.doi.org/10.1016/j.atmosres.2014.05.026

reasons, in-flight icing can be a significant hazard to all forms of aircraft (Politovich, 1996; Fernández-González et al., 2014) and its detection is a high priority for the Federal Aviation Administration as well as the commercial and general aviation community.

Multi-channel microwave radiometers have been developed and utilized over the last few decades to provide continuous measurements of liquid profiles and other variables of state (Heggli et al., 1987; Solheim et al., 1998; Ware et al., 2013). Another method of detecting liquid profiles involved a balloon-borne instrument based on vibrating wire technology (Hill and Woffinden, 1980) to derive profiles of SLW, which was developed by the ATEK Corporation. Previous work by Ware et al. (2003) showed that over 24 cases where vibrating wire sondes were launched near a profiling radiometer that on average the height of the liquid layers matched 50% of the time between sonde and radiometer even though significant differences existed between the liquid measuring techniques of each instrument. This SLW sonde technology never gained widespread adoption as the developer did not make the technology available for large-scale production and commercialization. A prototype SLW sonde has recently been developed by Anasphere Inc. with support by The National Aeronautical and Space Administration (Bognar et al., 2011) that uses the same vibrating wire principles and vibrational sensing technology as the ATEK Corp. sondes while incorporating other technical improvements. The purpose of this effort was to launch sondes into cold-season stratiform cloud which contained SLW and compare the resulting supercooled liquid water content (SLWC) profiles to liquid water path (LWP) and SLWC derived from ground-based radiometers. Section 2 is a description of the data sources utilized by this study for atmospheric observations. Section 3 is a methods used section. Section 4 describes the theory and design of the SLWC sondes. Section 5 details two SLWC sonde balloon launches conducted on March 7th, 2012. Section 6 is a discussion on sources of error in the SLWC sonde/radiometer comparison and Section 7 are conclusions based on this study's findings.

2. Observations

2.1. Supercooled liquid sonde

SLWC sondes were launched near a radiometer in cases with known SLWC, whose presence was verified with Pilot Reports of in-flight icing. The theory and practice of profiling SLWC with vibrating wire sondes attached to balloon-borne radiosondes are discussed in detail in Section 4.

2.2. Radiometer

A Radiometrics MP-3000A Series 35-channel microwave radiometer was located on the roof of Radiometrics Corporation's two-story office building located in North Boulder, CO. The passive microwave radiometer, the derived LWP, SLWC, humidity and temperature profiles are described by Solheim et al. (1998), Ware et al. (2003), Knupp et al. (2009), Cimini et al. (2011), Gultepe et al. (2012) and Friedrich et al. (2012). LWP can be calculated using closed retrieval algorithms and SLWC profiles are computed by building a training set of 10,000 historical radiosonde profiles from Denver and inverting the meteorological fields by computing the associated brightness temperatures with a radiative transfer model. Previous studies found that the radiometer LWP retrieval accuracy was better than 15% for a broad range of cloudy conditions (Westwater, 1978) and that there was no dependency on the sampled drop size (Westwater, 1978; Snider et al., 1980). Sampling volume considerations between the radiometer and the SLWC sonde are addressed in the Section 6 Discussion.

For this field study, the radiometer was programmed to collect brightness temperatures from zenith and off-zenith (15 degree elevation) north and south observations. Retrievals only from the northerly observation direction were used in the analysis, as that was the approximate mean direction of travel of the sondes. At 15 degrees elevation, the radiometer is viewing along an optical path that is equivalent to the depth of four atmospheres, as opposed to one atmosphere at zenith. At this low viewing angle, the radiometer's individual channel weighting functions become maximized in the lowest few kilometers and do so much closer in altitude to each other, which acts to increase the sensor's resolution in the lowest atmospheric levels (Xu et al., 2014). The low elevation viewing angle also means the sensor is viewing through the nearly vertical sides of the hydrophobic radome, which further mitigates the effects of precipitation on the detected brightness temperatures.

2.3. Pilot reports

When pilots visually detect icing on their aircraft, they can choose to voluntarily call in a Pilot Report to an air traffic controller that specifies a subjective icing severity ('null', 'trace', 'light', 'light–moderate', 'moderate', 'moderate–severe' and 'severe'), icing type ('rime', 'clear' or 'mixed'), reported altitude, air temperature, hazard location coordinates and other meteorologically relevant fields. Known deficiencies in the quality of these data such as occasional locational misreporting, decoding errors, subjective severity categorization, and severity dependence on aircraft type and size are detailed in Kelsch and Wharton (1996).

3. Method

In order to make a direct comparison between sonde and radiometer SLWC, several physically realistic constraints were applied to the raw neural network liquid profile retrieval derived from the radiometer. First, the radiometer temperature profile is adjusted to saturate the relative humidity with respect to liquid inside cloud. Second, cloud-top infrared temperature values from the Geostationary Earth-Orbiting Satellite infrared channel values are used to constrain the vertical extent of liquid detected by the radiometer. Third, liquid densities less than 0.03 g m^{-3} were considered to fall within the neural network noise level and therefore were adjusted to zero. Finally, the radiometer SLWC profile was normalized so that the integral of the profile was equal to the radiometer retrieved LWP value.

4. Theory and design of SLW sondes

Working from previous designs (Hill and Woffinden, 1980) which had been offered commercially at one time, instrument development began with the intent to employ a new version of a vibrating wire sensor for SLWC measurement. The goals for the design reported in this paper were to make the sensor smaller and lighter than the preceding design, to improve performance, and to reduce power consumption. None of the underlying physical principles relating ice accretion to vibrational frequency have been affected by the updates involved with this updated sensor since Hill and Woffinden's work. The following subsections detail the improvements that were made on the previous vibrating wire sondes. Anasphere's prototype SLWC sonde is illustrated in Fig. 1.

4.1. Wire

The design point for the new sensor was a 90-mm length of 0.61-mm diameter steel piano wire- the same wire sensing element as used in the earlier sensor. This was done to ensure comparability between the new and old sensors, and because that particular wire diameter was chosen by Hill for its efficiency in collecting a wide range of droplet sizes under typical balloon ascent speeds.

4.2. Vibration excitation

This is another area in which the new design substantially changed from the preceding design. Rather than continuously exciting a vibration, the choice was made to instead pluck the wire using a magnet attached to the end of a servo arm. The servo arm brings the magnet into contact with the wire, and then as it is rotated back, the wire eventually springs free. This action cycle is repeated roughly every three seconds. This approach also reduces the power consumption and mass of the overall sensor as compared to earlier designs.

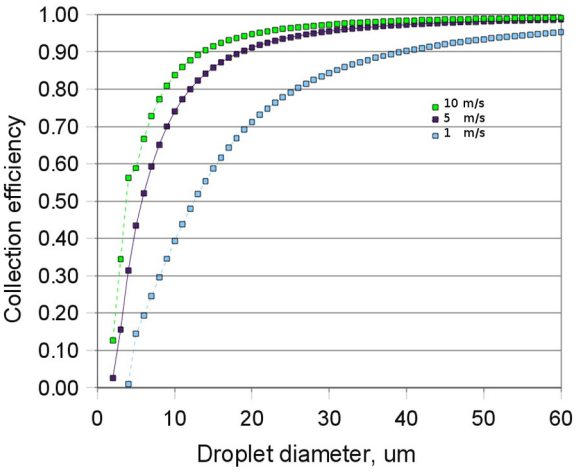

Fig. 2. Collection efficiencies for 1, 5 and 10 m s^{-1} relative wind speed and 0.6 mm wire diameter.

4.3. Vibration sensing

A polymer piezoelectric sensor is used to sense the vibration of the wire. A sandwich construction method consisting of a layer of silicone rubber, followed by the sensor, then the wire, and finally another layer of silicone rubber is used. The entire sandwich is contained between two Delrin® blocks. The wire is prevented from shifting by having a short right-angle bend at one end which yields a sharp point that is embedded in the silicone rubber. There is approximately 20 mm of wire held against the piezoelectric sensing material, which is in addition to the exposed 90-mm length. This sensing

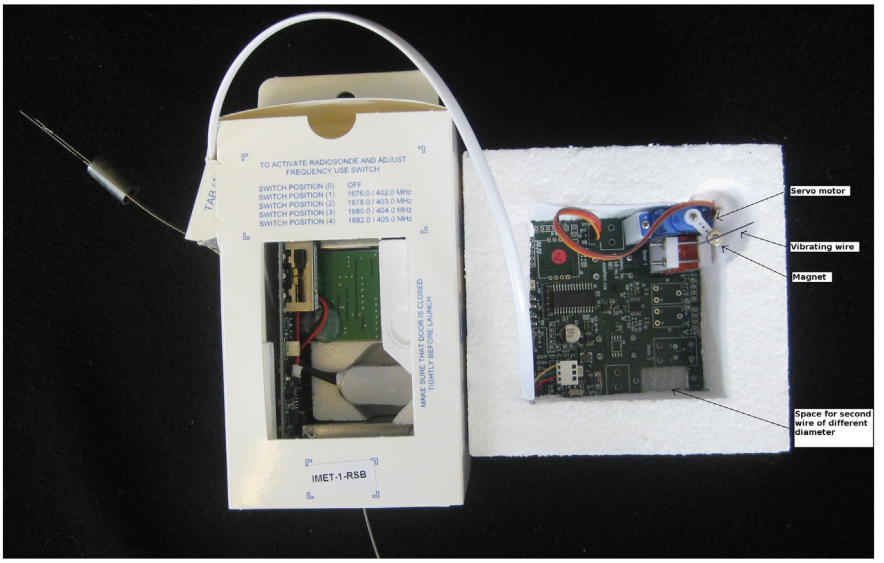

Fig. 1. SLW sonde (right) connected in series to an i-Met radiosonde (left).

method is purely passive and represents one area in which power consumption was reduced as compared to preceding designs.

4.4. Physical and electrical specifications

The overall sensor printed circuit board is 3 × 3 inches in size. Mass of a single complete sensor is 46.6 grams and the two lithium AAA cells used to power the sondes add an additional 15.2 grams. When packaged for flight, the sensor is housed in a Styrofoam box with 2.5 cm walls all around except for the lid, which consists of a 0.08 cm thick polystyrene sheet with a small hole cut in it for the sensor wire. In this configuration, the SLW sonde has a mass of 100 grams with batteries.

4.5. SLWC calculation

In the Hill system, a length of wire was exposed to the ambient environment and excited into vibration with an electromagnet, and the resulting vibration frequency of the wire was measured. The exposed wire on a SLWC sonde vibrates at the same base frequency every time it is plucked when the wire is free of ice. As ice builds up from freezing of impacting SLWC, the vibration frequency of the wire was reduced. Solid particles do not adhere to the wire and thus are not a factor in the SLWC calculation. Using mathematical approaches described by Hill and Woffinden (1980) and with subsequent refinements described in Hill (1994), the supercooled liquid water concentration was computed using (1).

$$SLWC = -\frac{2b_0 f_0^2}{\varepsilon D \omega f^3}\frac{df}{dt} \tag{1}$$

where f_0 is the pre-launch un-iced wire frequency, ε is the drop collection efficiency, D is the wire diameter, ω is the air velocity relative to the wire, f is the wire frequency at a given time during flight, df/dt is the time rate of change in frequency and b_0 is a measure of steel wire weight per unit length as 0.0224 g cm^{-1} (for the tested configuration). The drop collection efficiency for the specific wire diameter of 0.61 mm used on the SLWC sonde was computed using the method discussed in Lozowski et al. (1983) and is shown for a relevant range of drop diameters in Fig. 2. In order to illustrate how collection efficiency varies over the reasonable range of mean

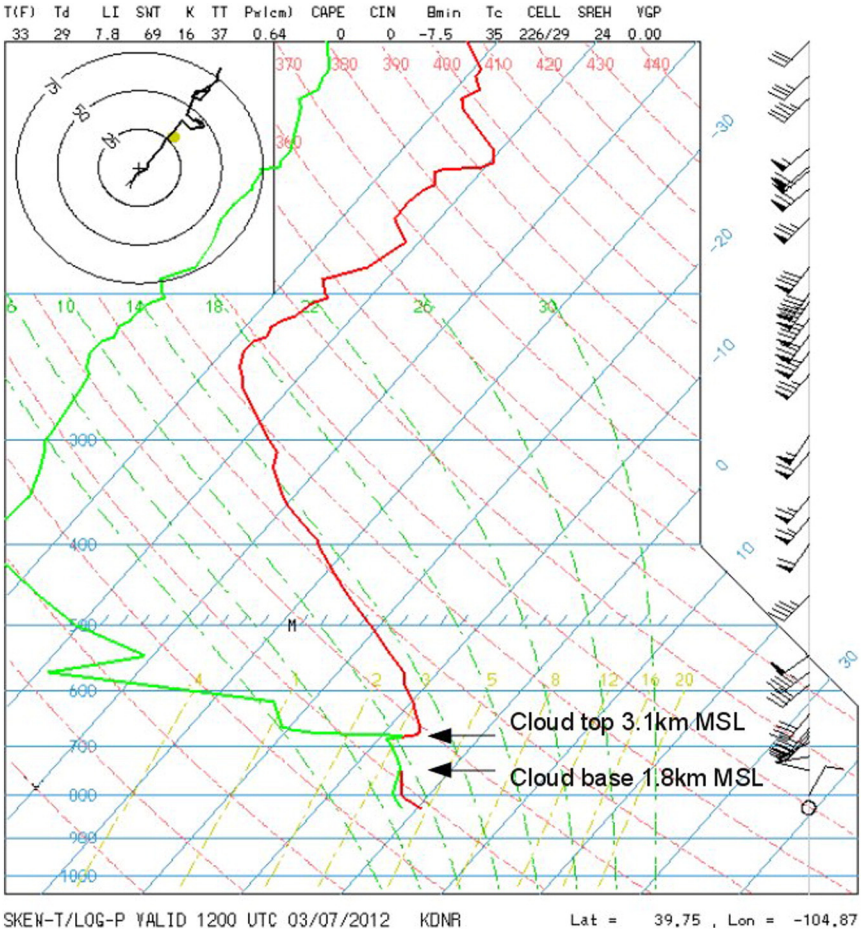

Fig. 3. Skew-T plot of temperature (red) and dewpoint temperature (green) from the National Weather Service radiosonde launched from Denver at 12 Z on March 7th, 2012. (For interpretation of the references to colour in this figure legend, the reader is referred to the web of this article.)

Table 1
Pilot reported relevant icing fields within 50 km of the SLW sonde launch locations at Boulder, Colorado on March 7th, 2012.

Hour	Min	Icing severity	Report altitudes [km MSL]	Air temp [deg C]
13	55	Moderate	Unknown	−19
14	0	Moderate	2.8–3.3	−22
14	35	Light	Below 3.3	−21
15	3	Moderate	2.4–3.3	−18
15	21	Light-Moderate	2.2–3.1	−19
15	52	Light-Moderate	Below 3.0	−21
16	25	Light	2.0–2.7	−19

relative velocities, three mean velocities from 1 to 10 m s^{-1} including the mean relative rate of 5 m s^{-1} are shown.

4.6. Data and telemetry

The Anasphere SLWC sonde utilizes the XDATA digital interface developed by researchers at the National Oceanic and Atmospheric Administration and used on Intermet's IMET-1 radiosonde. The data is sent down via a wireless transmitter on the radiosonde at 403 MHz at 1200 baud, whose sampling rate can be varied by the user and can be as fast as one sample every second. Due to the action cycle of the magnet mounted on the servo arm discussed in Section 4.2, a sampling rate of one sample every three seconds was most practical for the SLWC sonde. Lower rates would entail more repeated data values and higher rates could mean skipped data points.

The digital radiosonde interface was also created by researchers at the National Oceanic and Atmospheric Association and is particularly critical due to the amount of data generated by this sensor. The iMET-1 radiosonde can transmit roughly 100 XDATA bytes of data per second from external instruments as well as the pressure, temperature, humitidy, and GPS data it is already transmitting. While the SLWC sonde frequency data only consists of several bytes, this still overwhelms any typical (and especially analog) radiosonde interface. The low receiving station cost, the compatability with the SLW sonde's XDATA format, the amount of data it can send down per second, and the flexibility and ease of use of the researcher software interface make the iMET radiosonde the easiest system to use for external instrumentation.

5. Field testing results: March 7th, 2012

On this date, two SLWC sondes were launched within two hours of each other into significant SLWC aloft. A cutoff upper level low over the Four Corners and an associated surface low over the Denver area brought a cold front through all of

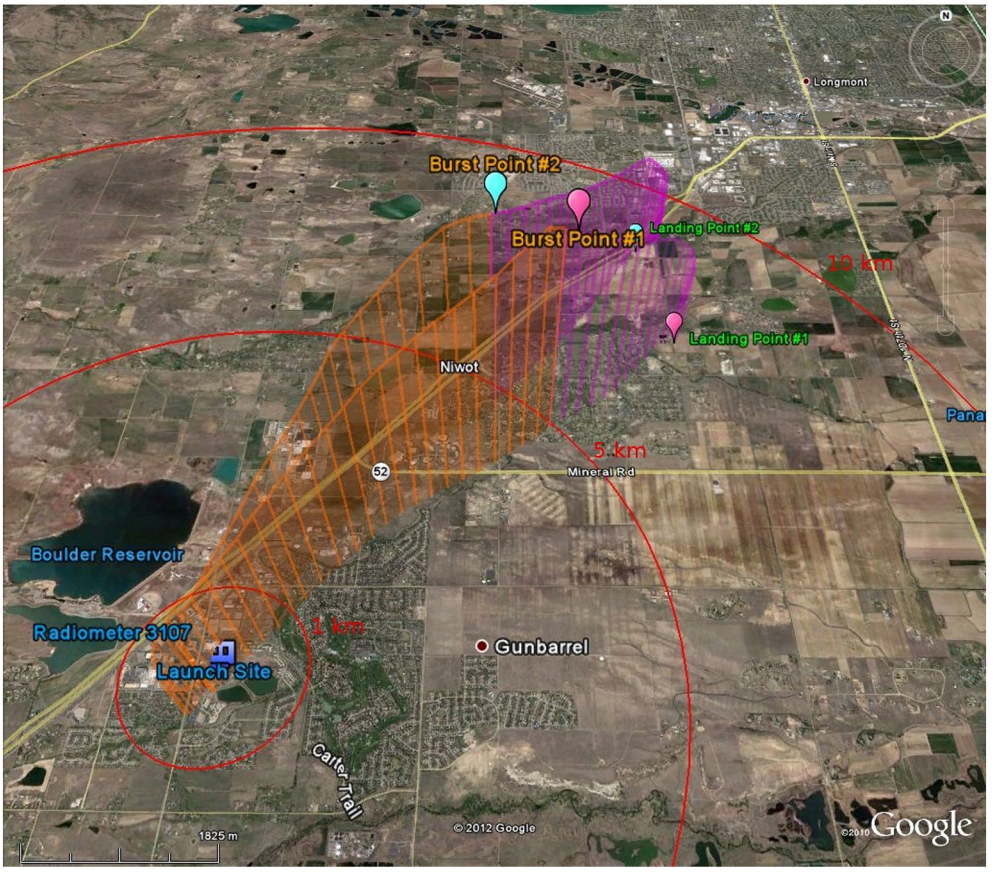

Fig. 4. Launching location (lower left), flight tracks and landing locations for SLW sonde flights #1 and #2 on March 7th, 2012. Radiometer location in blue text. 1, 5 and 10 km range rings in red.

Northeast Colorado by 12Z on March 7th. The 12 Z balloonsonde profile launched from near Denver International Airport (Fig. 3) showed a subfreezing profile, shallow upslope near the surface and an adiabatically saturated stratiform cloud layer from 1.8 km above the surface up to 3.1 km MSL caused by orographic and dynamical liftling of the lower atmospheric layers. Above that cloud layer was a significant temperature inversion and likely a stark cloud-to-clear air boundary. The orographic upslope flow led to the adiabatic layer lifting and the resulting condensation of available moisture in the cloud layer below the inversion into increasing liquid amounts. This process eventually led to the production of freezing drizzle (discussed further in Section 6). Moderate freezing drizzle was observed at the ground launch site in North Boulder from before 13:30 Z to after 16:30 Z. Denver's automated weather system reported 'unknown precipitation type', 'fog' and 'mist' during the flight times. Many icing PIREPs were recorded within 50 km of the SLW sonde launch site during the period of 13:55 and 16:30 Z (Table 1), including two 'light', two 'light-to-moderate' and three designated as 'moderate' icing severities.

Preparation of the balloon, sonde package and data acquisition system began at around 13:30 Z and was completed by 14:00 Z. Fig. 4 shows the launch and landing locations, flight tracks and radiometer locations for the two flights made during this case. The following subsections detail how the observed wire frequency change with time from the two sonde flights was converted to a SLWC profile, and include a comparison of the sonde SLWC to the SLWC derived from the nearby radiometer. One significant issue that occasionally can occur with ground-based radiometers is the formation of ice on the hydrophobic radome when freezing precipitation is present. On this date, a visual inspection of the radome was performed before and after each sonde launch to confirm that ice accretion was not occurring. Any ice accretion would occur on the radiometer in the windward direction and would cause differences in the zenith, 15 degree elevation northward and 15 degrees southward retrievals—none of which were observed during this event. Only retrievals from the radiometer's 15 degree elevation observations facing directly toward north azimuth were used for the following comparisons because it matches approximately to the mean direction of travel of the sondes.

5.1. Sonde profile #1

The first sonde was launched at 14:07 Z and landed at 14:25 Z, lasting a total of 18 minutes. An electronic cutdown device burned through the nylon string at 4.9 km MSL (3.3 km AGL), and the sonde package descended to the ground by parachute. Several PIREPs, mostly of 'moderate' severity, were reported in the Denver area around the sonde launchtime. Fig. 5 shows the ascent profiles of SLWC sonde frequency versus altitude (left window, blue) and an 11-point moving average of frequency versus altitude (red). The frequency decreases at an increasing rate from the surface up to 3.2 km MSL, due to increasing accretion of SLWC onto the vibrating wire. Above 3.2 km MSL, the frequency increases all the way up to the cutdown height as

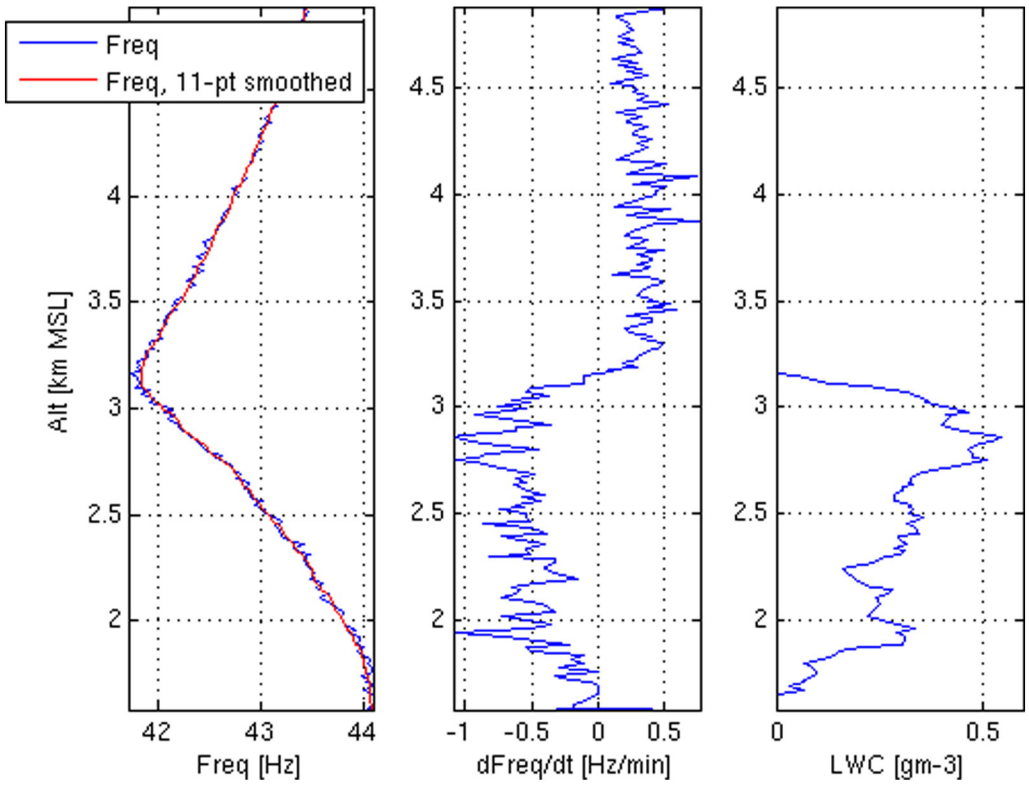

Fig. 5. Ascending profiles of wire frequency (blue, left) and smoothed frequency (red, left), rate of frequency change per minute (center) and derived LWC (right) for the first launch that began at 14:07 Z on March 7th, 2012. (For interpretation of the references to colour in this figure legend, the reader is referred to the web of this article.)

accreted ice was reduced by sublimation of ice directly to water vapor. The smoothed frequency profile is converted to a change in frequency per unit time plot (center window, [Hz min^{-1}]), which was negative and decreases to a minimum at 2.8 km then increases rapidly with height to positive values above 3.2 km MSL. Using Eq. (1), the change in frequency profile was used to compute SLWC (right window, [g m^{-3}]).

A temperature profile collected by the radiosonde (Fig. 6, left window, solid blue) indicates that the cloud producing the freezing drizzle is not the result of parcels rising and cooling from the lifting condensation level (LCL) at cloud base where the air first becomes saturated. For this mode of cloud development to exist, the lapse rate of the temperature profile within the cloud would need to be at the moist adiabatic lapse rate (shown as a blue dashed line). The only way to produce this LWC profile with the radiosonde temperature profile is with lifting of multiple layers. A 3° C inversion in the temperature, measured by the radiosonde at 3.2 km MSL, created a highly stable layer which capped the clouds' vertical development. Sonde-derived SLWC values increase rapidly beginning a few hundred meters above the surface and generally increases to a maximum value of around 0.5 g m^{-3} near the cloud top. In this manner, the sonde-derived SLWC profile is reasonable if the lifted air layer that was producing the upper portion of the cloud had more moisture in it than the portion that created the lower portion of the cloud. SLWC falls off rapidly near the temperature inversion at 3.2 km MSL, as does the radiosonde-derived relative humidity (right window, [%]). A generalized SLWC profile that steadily increases with height up toward cloud top and then falls off rapidly with a stably capped temperature inversion has been frequently observed in previous icing research flight studies (Rasmussen et al., 1992; Politovich, 1996; Ikeda et al., 2007; Vidaurre et al., 2011).

SLWC can exist below 2 km when the relative humidity reported by the radiosonde is below 80% because supercooled large drizzle drops are falling from the cloud are making it to the surface, as evidenced by the observed freezing drizzle mentioned previously. As the relative humidity below cloud base is below saturation, these drops are out of equilibrium with their surroundings and are necessarily losing mass and volume to evaporation, albeit probably very little. Another factor is response time lag involved with the rapidly rising radiosonde's measurement of the relative humidity. Overall, the characteristics of the sonde-derived SLWC profile conform to the conditions determined by the radiosonde meteorological fields.

Profiles from the radiometer, which was collecting data on the roof of the Radiometrics building, are overlaid on the sonde SLWC plot (center window). The shape and maximum

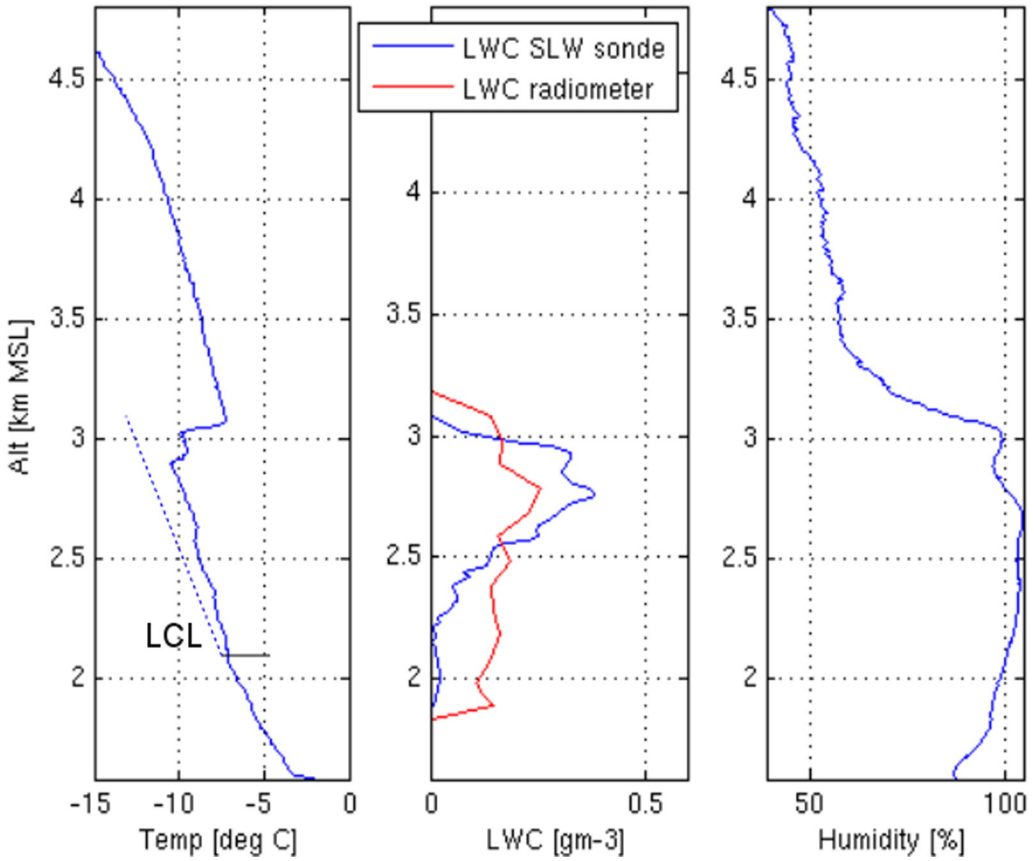

Fig. 6. Ascending profiles of radiosonde temperature (left), SLW sonde derived LWC (blue, center) and radiometer derived LWC (red, center) and radiosonde relative humidity (right) for the first launch that began at 14:07 Z on March 7th, 2012. (For interpretation of the references to colour in this figure legend, the reader is referred to the web of this article.)

magnitude of the radiometer SLWC profile are somewhat different from the sonde profile. The sonde has a more classic shape of generally increasing SLWC values with a maximum just below the cloud top inversion, while the radiometer has a maximum near the middle of the cloud layer at 2.2 km MSL and tapers off gradually above and below the height of maximum LWC. Differences in the SLWC sonde and radiometer derived profiles are most likely due to the relative insensitivity of the radiometer to vertical SLWC resolution and smoothing due to the relatively large field of view of the radiometer (See Section 6). Due to the significant differences in measuring methods and volumes between the sonde and radiometer, neither is to be considered 'correct' or 'better' than the other. Both instruments are providing part of the answer to the question of what is the SLWC profile in this in-flight icing case.

The LWP computed from the sonde flight #1 ascent profile was 0.43 mm, compared to mean values during the ascent times of 0.51 mm liquid derived from the rooftop radiometer at the time of launch. These radiometer values relative to the SLWC sonde were generally comparable to previous studies (Westwater, 1978; Westwater et al., 2001) which showed radiometer LWP values within +/−15% of in-situ measured ILW.

5.2. Sonde profile #2

The second balloonsonde was launched at 15:57 Z and landed at 16:15 Z, lasting a total of 18 min. An electronic cutdown device burned through the nylon string at 4.8 km MSL (3.2 km AGL), and the sonde package descended to the ground by parachute. Several PIREPs, mostly of 'light' and 'light–moderate' severity, were reported in the Denver area around the sonde launchtime. Fig. 7 shows the ascent profiles of SLWC sonde frequency versus altitude (left window, blue) and an 11-point moving average of frequency versus altitude (red). The frequency decreases with an increasing rate starting at 2.5 km MSL up to 3.1 km MSL, due to accretion of SLWC onto the vibrating wire. Above 3.1 km MSL, the frequency increases all the way up to the cutdown height as accreted ice is reduced by sublimation. The smoothed frequency profile is converted to a change in frequency per unit time plot (center window, [Hz min^{-1}]), which decreases to a minimum at 2.8 km then increases rapidly with height to positive values above 3.1 km MSL. Using Eq. (1), the change in frequency profile is used to compute SLWC (right window, [g m^{-3}]).

A 3° C inversion in the temperature measured by the radiosonde at 3.1 km MSL (Fig. 8, left window) created a highly stable layer which caps the cloud tops. Once again, the temperature profile is sub-moist adiabatic (dashed blue line), indicating the cloud depth is not solely the product of parcel ascent from the LCL but rather was produced from layer lifting. With this later launch, the lower portion of the SLWC profile is seen to have significantly eroded (right window, [%]), with only a small remnant of the former relative maxima at 2 km MSL remaining. The sonde-derived SLWC values increase rapidly above 2.5 km MSL and the profile generally increases with height towards the cloud-top temperature inversion, falling

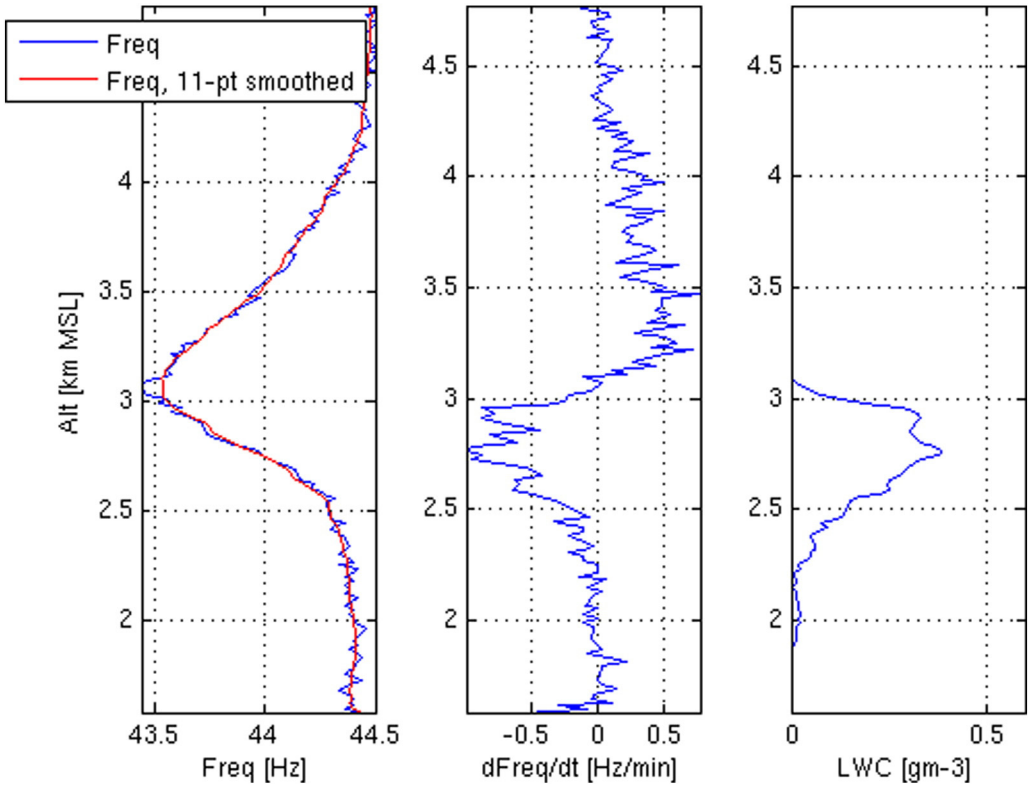

Fig. 7. Ascending profiles of wire frequency (blue, left) and smoothed frequency (red, left), rate of frequency change per minute (center) and derived LWC (right) for the second launch that began at 15:57 Z on March 7th, 2012. (For interpretation of the references to colour in this figure legend, the reader is referred to the web of this article.)

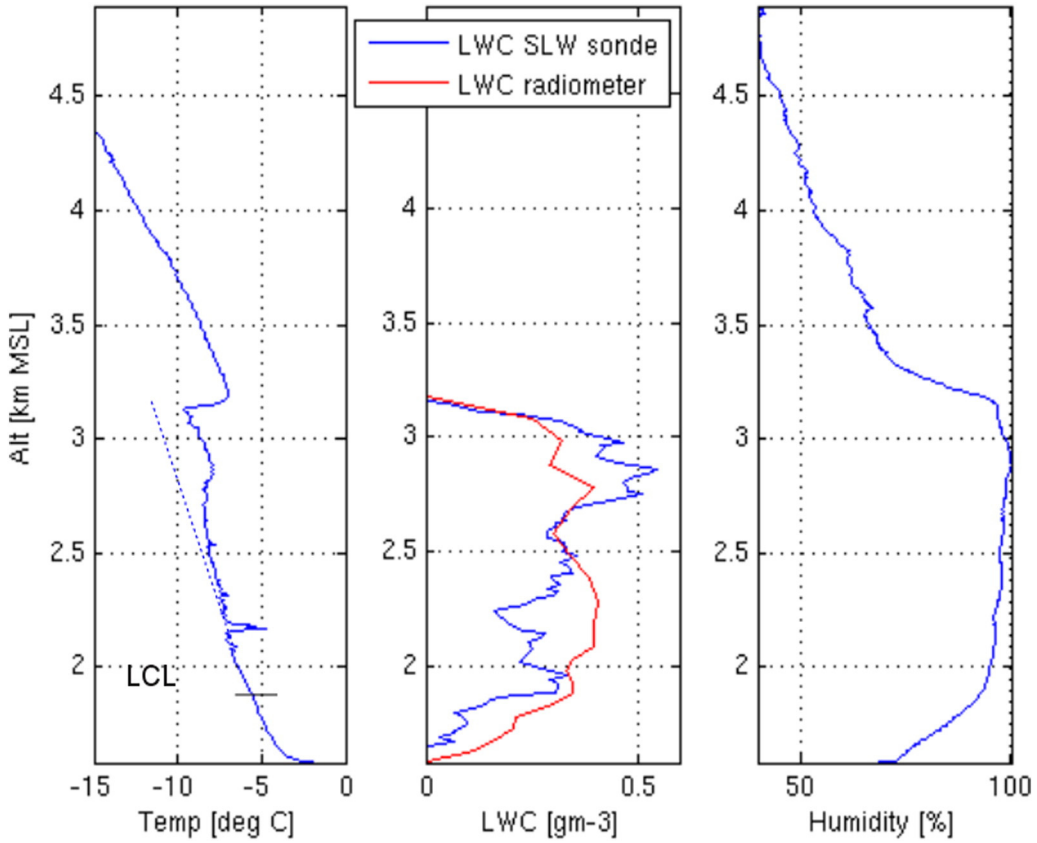

Fig. 8. Ascending profiles of radiosonde temperature (left), SLW sonde derived LWC (blue, center) and radiometer derived LWC (red, center) and radiosonde relative humidity (right) for the second launch that began at 15:57 Z on March 7th, 2012. (For interpretation of the references to colour in this figure legend, the reader is referred to the web of this article.)

rapidly to zero above 3 km MSL. The maximum value is about 0.35 g m^{-3} near the cloud top. The SLWC from the sonde falls off rapidly near the temperature inversion at 3.1 km MSL, as does the radiosonde-derived relative humidity. The SLWC is also seen to be confined to heights where relative humidity as measured by the radiosonde is greater than 80%, which is corroborated by previous studies (Chernyk and Eskridge, 1996). Incidently, relative humidity values above 100% recorded while in cloud are likely due to a slight calibration error with the radiosonde. As with the first sonde launch, the characteristics of this sonde-derived SLWC profile conform to the conditions determined by the radiosonde meteorological fields. In contrast to the sonde SLWC, the radiometer liquid values continue several hundred meters above the capping temperature inversion and where relative humidity is on the order of 60 to 70%. These SLWC differences are attributable to differences in resolutions and sensing volumes of the two measurement platforms.

The LWP computed from the sonde flight #2 ascent profile was 0.17 mm, compared to a value during the ascent time of 0.22 mm liquid derived from the rooftop radiometer. These radiometer values were once again comparable to previous studies which showed radiometer LWP values within +/− 15% of in-situ measured LWP. The most likely reason for the relatively minor discrepancies include differences in sampling volumes between radiometer and sonde.

6. Discussion

Although this technology development effort has afforded only the two cases discussed in this work to date, important considerations on the sonde and radiometer SLWC profiles (Figs. 6 and 8) can be made. Table 2 shows the absolute difference (LWC_{diff}) in sonde SLWC (LWC_S) and radiometer SLWC (LWC_R) from sonde flights #1 and #2 in units of g m^{-3} shown in 200 m altitude increments from the surface to above the cloud tops. The absolute differences are also 'normalized' by the SLWC sonde value at each altitude. It can be seen that the sonde SLWC exceeds that of the radiometer in the upper portion of the cloud layer. Radiometer SLWC was much higher in the lower portions of the cloud, especially during flight #2 when the freezing drizzle event was observed to be decaying.

The two methods of providing SLWC profiles each sample the environment with significantly different spatial and temporal resolutions. The microwave channels used by the r-ciometer have between 4 and 6 degree beamwidths, thus averaging over an increasingly expanding cone of influence with distance from the passive microwave receiver. Brightness temperatures and resulting LWP and SLWC are integrated roughly every 25 seconds for the sampled volume. The SLWC sonde is sampling only the relative airflow in direct proximity to its vibrating wire every few seconds as it

Table 2
Difference in absolute values of LWC from sonde and radiometer [g m^{-3}], normalized SLW difference [unitless]and radiosonde relative humidity [%] from sonde flights #1 (columns 2-4) and #2 (columns 5-7) on March 7th, 2012.

	Flight #1			Flight #2		
Altitude [km MSL]	$LWC_S - LWC_R$	LWC_{diff}/LWC_s	RH [%]	$LWC_S - LWC_R$	LWC_{diff}/LWC_s	RH [%]|
3.2	0	0	65	0	0	74
3	0.13	0.3	99	−0.02	−0.14	100
2.8	0.1	0.21	99	0.11	0.31	99
2.6	−0.03	−0.14	98	0.07	0.3	102
2.4	−0.08	−0.27	98	−0.09	−1.5	102
2.2	−0.17	−0.77	96	−0.16	−16	102
2	−0.1	−0.4	94	−0.09	−4.5	99
1.8	−0.14	−1.56	86	0	0	96
1.6	0	0	75	0	0	86

is moved horizontally by the mean wind and vertically by buoyancy and vertical atmospheric motions. As the radiometer was oriented directly north and the balloon trajectory was to the north-north east, the differing sampling volumes may not have completely overlapped. Without research aircraft flights outfitted with SLWC and particle probes, we cannot truly say if one or the other methods of deriving SLWC is right or wrong. The best we can do is admit that both profiles are microphysically reasonable given the icing PIREPs and local observations of freezing drizzle. Several previous studies involving in-situ aircraft profiles of SLWC during the AIRS-II, (Reehorst et al., 1995), WISP-04 (Politovich et al., 1995) and IMPROVE-2 (Ikeda et al., 2007) field campaigns provide ample evidence for the significant frequency of occurrence of 'wedge-shaped' SLWC profiles that reach a maximum values near cloudtop inversions. All three studies postulated that layers were being lifted adiabatically in an environment that was relatively 'clean' of condensation nuclei, allowing the available water vapor to condense and remain as supercooled liquid in increasing amounts until reaching the cloudtop temperature inversion as an upper boundary. Supercooled drops that grow large enough in mass can overcome the dynamical lift and fall out as freezing drizzle, as is occurring in this event.

7. Conclusion

Knowledge of the presence, amount and distribution with height of supercooled liquid in the atmospheric column is important to aviation safety, advancing understanding of meteorological microphysics, hydrological studies and numerical weather prediction modeling. A new generation of advanced vibrating wire SLWC sondes has been developed by Anasphere Inc. and tested by NASA and NCAR for these purposes. Two weather balloons with SLWC sonde/radiosonde instrument packages were launched during a significant stratiform freezing drizzle event on March 7th, 2012. The instruments were launched at the location of a multichannel microwave radiometer profiler at Boulder, CO in order to compare their respective derived SLWC and ILW profiles.

Overall, the SLWC sondes produced meteorologically consistent and reasonable SLWC profiles in terms of magnitude and profile shape, and the LWP values were very similar to values derived from the radiometer. The derived profiles from the SLWC sondes matched characteristics of SLWC observed in many previous research flights such as gradually increasing SLWC values with height with maximum near the top of the profile and rapid decrease in SLWC values near the cloud top inversion associated with large drop in-flight icing events. Ideally, these SLWC sonde flights would be validated with research aircraft flights outfitted with SLW and particle probes to provide in-situ verification of the magnitude of SLW through a given profile, but such flights are currently not possible due to the entailed financial cost. Until such a field campaign can be conducted, comparison to ground-based radiometry and pilot reports of icing are the best available sources of SLWC verification.

The radiometer measured LWC profiles exhibited LWP values within +/− 15% of the SLW sonde derived values. The LWP differences are well within uncertainty resulting from sampling volume and location mismatches. Radiometer profiles maximized in the middle of the cloud and the sensed liquid was spread deeper into the atmosphere, even somewhat above cloud top inversions.

In this initial testing phase, the SLWC sonde proved to be stable, durable and exhibited sufficient time resolution in the change in vibration frequency proving it capable of resolving narrow stratiform SLWC layers and significant SLWC gradients. It is not yet known how well the sondes would capture SLWC values in non-cold season convective clouds where SLW is the result of sometimes strong updrafts. The convective weather scenario needs to be studied in future field campaigns. The new SLWC sonde also appears capable measuring a relevant range of drop sizes that includes the lower end of the supercooled large drop range, whose sizes are difficult for aircraft probes to measure. Future work includes further icing wind tunnel testing and free-atmosphere testing in various SLWC weather scenarios. Future versions of SLWC sonde flight packages may include a second wire module of different diameter to possibly derive drop size distributions through differential wire collection efficiencies.

Acknowledgments

This research is sponsored by the NASA Aviation Safety Program under the Atmospheric Environment Safety Technologies (AEST) project. The sensor development was supported in part by NASA SBIR Phase I contract NNX11CD74P.

References

Bognar, J., Abdo, S., Baker, K., Seitel, T., 2011. Cloud Liquid Water Content Sensor for Radiosondes. NASA SBIR Phase I Final Report.

Chernyk, I. And, Eskridge, R., 1996. Determination of cloud amount and level from radiosonde soundings. J. Appl. Meteorol. 35, 1362–1369.

Cimini, D., Campos, E., Ware, R., Albers, S., Graziano, G., Oreamuno, J., Joe, P., Koch, S., Cober, S., Westwater, E., 2011. Thermodynamic Atmospheric Profiling during the 2010 Winter Olympics Using Ground-based Microwave Radiometry. Trans. Geosci. Remote Sens. 49, 4959–4969.

Fernández-González, S., Sánchez, J., Gascón, E., López, L., García-Ortega, E., Merino, A., 2014. Weather features associated with aircraft icing conditions: a case study. Sci. World J. 2014, 1–17.

Friedrich, K., Lundquist, J., Aitken, M., Kalina, E., Marshall, R., 2012. Stability and turbulence in the atmospheric boundary layer: An intercomparison of remote sensing and tower observations. Geophys. Res. Lett. 39, 1–6.

Gultepe, I., Bendix, J., Klemm, O., Eugster, W., Cermak, J., 2012. Fog and dew observations and modeling: Introduction. Pure and Applied Geophysics, 169. Birkhauser Publishing, pp. 765–766.

Heggli, M., Rauber, R., Snider, J., 1987. Field evaluation of a dual-channel microwave radiometer designed for measurement of integrated water vapor and coud liquid water in the atmosphere. J. Atmos. Ocean. Technol. 4, 204–213.

Hill, G.E., 1994. Analysis of Supercooled Liquid Water Measurements Using Microwave Radiometer and Vibrating Wire Devices. J. Atmos. Ocean. Technol. 11, 1242–1252.

Hill, G.E., Woffinden, D., 1980. A Balloonborne Instrument for the Measurement of Vertical Profiles of Supercooled Liquid Water Concentration. J. Appl. Meteorol. 19, 1285–1292.

Ikeda, K., Rasmussen, R., Hall, W., Thompson, G., 2007. Observations of freezing drizzle in extratropical cyclonic storms during IMPROVE-2. J. Atmos. Sci. 64, 3016–3043.

Kelsch, M., Wharton, L., 1996. Comparing PIREPs with NAWAU turbulence and icing forecasts: Issues and results. Weather Forecast. 11, 385–390.

Knupp, K., Ware, R., Cimini, D., Vandenberghe, F., Vivekanandan, J., Westwater, E., Coleman, T., 2009. Ground-Based Passive Microwave Profiling during Dynamic Weather Conditions. J. Atmos. Ocean. Technol. 26, 1057–1073.

Lozowski, E.P., Stallabrass, J.R., Hearty, P.F., 1983. The Icing of an Unheated, Nonrotating Cylinder Part I: A Simulation Model. J. Clim. Appl. Meteorol. 22, 2053–2062.

Politovich, M.K., 1996. Response of a research aircraft to icing and evaluation of severity indices. J. Aircr. 33, 291–297.

Politovich, M.K., Bernstein, B., 1995. Production and depletion of supercooled liquid water in a Colorado Winter Storm. J. Clim. Appl. Meteorol. 34, 2631–2648.

Rasmussen, Politovich, R.M., Marwitz, J., Sand, W., McGinley, J., Smart, J., Pielke, R., Rutledge, S., Wesley, D., Stossmeister, G., Bernstein, B., Elmore, K., Powell, N., Weswater, E., Stankov, B., Burrows, D., 1992. Winter Icing and Storms Project (WISP). Bull. Am. Meteorol. Soc. 73, 951–974.

Reehorst, A., Brinker, D., Ratvasky, T., Ryerson, C., Koenig, G., 1995. The NASA Icing Remote Sensing System. AMS Annual Conference preprint.

Snider, J., Guiraud, F., Hogg, D., 1980. Comparison of cloud liquid content measured by two independent ground-based systems. J. Appl. Meteorol. 19, 577–579.

Solheim, F., Godwin, J., Westwater, E., Han, Y., Keihm, S., Marsh, K., Ware, R., 1998. Radiometric profiling of temperature, water vapor and cloud liquid water using various inversion methods. Radio Sci. 33, 393–404.

Vidaurre, G., Hallett, J., Rogers, D., 2011. Airborne Measurement of Liquid and Total Water Content. J. Atmos. Ocean. Technol. 28, 1088–1103.

Ware, R., Solheim, F., Carpenter, R., Güldner, J., Liljegren, J., Nehrkorn, T., Vandenberghe, F., 2003. A multi-channel radiometric profiler of temperature, humidity and cloud liquid. Radio Sci. 38, 1–13.

Ware, R., Cimini, D., Campos, E., Guiliani, G., Albers, S., Nelson, M., Koch, S., Joe, P., Cober, S., 2013. Thermodynamic and liquid profiling during the 2010 Winter Olympics. Atmos. Res. 132–133, 278–290.

Westwater, E., 1978. The accuracy of water vapor and cloud liquid determination by dual-frequency ground-based microwave radiometry. Radio Sci. 13, 677–685.

Westwater, E., Han, Y., Shupe, M., Matrosov, S., 2001. Analysis of integrated cloud liquid and precipitable water vapor retrievals from microwave radiometers during the Surface Heat Budget of the Arctic Ocean Project. J. Geophys. Res. 106, 32019–32030.

Xu, G., Ware, R., Zhang, W., Feng, G., Liao, K., Liu, Y., 2014. Effect of off-zenith observations on reducing the impact of precipitation on ground-based microwave radiometer measurement accuracy in Wuhan. Atmos. Res. 140–141, 85–94.